

Electromagnetic structure of $A=2$ and 3 nuclei in chiral effective field theory

Maria Piarulli*

Department of Physics, Old Dominion University, Norfolk, VA, 23529

E-mail: mpiar001@odu.edu

Luca Girlanda

*Dipartimento di Matematica e Fisica “E. De Giorgi”, Università del Salento,
INFN Sez. di Lecce, 73100, Italy*

E-mail: luca.girlanda@le.infn.it

Laura Elisa Marcucci

*Dipartimento di Fisica “E. Fermi”, Università di Pisa,
INFN Sez. di Pisa, 56127, Italy*

E-mail: marcucci@df.unipi.it

Saori Pastore

Department of Physics and Astronomy, University of South Carolina, Columbia, SC, 29208, USA

E-mail: pastore@mailbox.sc.edu

Rocco Schiavilla

Theory Center, Jefferson Laboratory, Newport News, VA, 23606, USA

Department of Physics, Old Dominion University, Norfolk, VA, 23529, USA

E-mail: schiavil@jlab.org

Michele Viviani

INFN, Sez. di Pisa, 56127, Italy

E-mail: viviani@pi.infn.it

The objective of this presentation is to provide a complete set of chiral effective field theory (χ EFT) predictions for the structure functions and tensor polarization of the deuteron and for the charge and magnetic form factors of ^3He and ^3H . The calculations use wave functions derived from high-order chiral two- and three-nucleon potentials and Monte Carlo methods to evaluate the relevant matrix elements. Predictions based on conventional potentials in combination with χ EFT charge and current operators are also presented. There is excellent agreement between theory and experiment for all these observables for momentum transfers up to $q \lesssim 2.0\text{--}2.5 \text{ fm}^{-1}$.

52 International Winter Meeting on Nuclear Physics - Bormio 2014,

27-31 January 2014

Bormio, Italy

*Speaker.

1. Introduction

Over the past two decades, chiral effective field theory (χ EFT), originally proposed by Weinberg in a series of papers in the early nineties [1], has blossomed into a very active field of research. The chiral symmetry exhibited by QCD severely restricts the form of the interactions of pions among themselves and with other particles. In particular, the pion couples to baryons, such as nucleons and Δ -isobars, by powers of its momentum Q , and the Lagrangian describing these interactions can be expanded in powers of Q/Λ_χ , where $\Lambda_\chi \sim 1$ GeV specifies the chiral-symmetry breaking scale. As a result, classes of Lagrangians emerge, each characterized by a given power of Q/Λ_χ and each involving a certain number of unknown coefficients, so called low-energy constants (LEC's), which are then determined by fits to experimental data (see, for example, the review papers [2], [3] and [4], and references therein). Thus, χ EFT provides, on the one hand, a direct connection between QCD and its symmetries, in particular chiral symmetry, and the strong and electroweak interactions in nuclei, and, on the other hand, a practical calculational scheme susceptible, in principle, of systematic improvement. In this sense, it can be justifiably argued to have put low-energy few-nucleon physics on a more fundamental basis.

Nuclear electromagnetic (EM) charge and current operators in χ EFT up to one loop have been first derived by Park *et al.* by using covariant perturbation theory [5, 6]. A few years ago, the derivation of EM charge and current operators in χ EFT has been reconsidered by Pastore *et al.* [7, 8, 9], and, in parallel, by Kölling *et al.* [10, 11]. Pastore *et al.* have used time-ordered-perturbation theory (TOPT) to calculate the EM transition amplitudes, while Kölling *et al.* have adopted the method of unitary transformation.

2. Nuclear current and charge operators up to one loop

The two-nucleon current (\mathbf{j}) and charge (ρ) operators have been derived in χ EFT up to one loop (to order eQ) in Refs. [8] and [9], respectively. In the following, we denote the momentum due to the external electromagnetic field with \mathbf{q} , and define

$$\mathbf{k}_i = \mathbf{p}'_i - \mathbf{p}_i, \quad \mathbf{K}_i = (\mathbf{p}'_i + \mathbf{p}_i)/2, \quad (2.1)$$

$$\mathbf{k} = (\mathbf{k}_1 - \mathbf{k}_2)/2, \quad \mathbf{K} = \mathbf{K}_1 + \mathbf{K}_2, \quad (2.2)$$

where \mathbf{p}_i (\mathbf{p}'_i) is the initial (final) momentum of nucleon i . We further define

$$\mathbf{j} = \sum_{n=-2}^{+1} \mathbf{j}^{(n)}, \quad \rho = \sum_{n=-3}^{+1} \rho^{(n)}, \quad (2.3)$$

where the superscript n in $\mathbf{j}^{(n)}$ and $\rho^{(n)}$ specifies the order eQ^n in the power counting. The contributions to the electromagnetic current and charge operators up to one loop are illustrated in Fig. 1 and Fig. 2, respectively. The leading order (LO) contributions $\mathbf{j}^{(-2)}$ and $\rho^{(-3)}$ consist of the single-nucleon current and charge operators:

$$\mathbf{j}^{(-2)} = \frac{e}{2m_N} [2e_{N,1}(q^2) \mathbf{K}_1 + i\mu_{N,1}(q^2) \boldsymbol{\sigma}_1 \times \mathbf{q}] \delta(\mathbf{p}'_2 - \mathbf{p}_2) + 1 \Leftrightarrow 2, \quad (2.4)$$

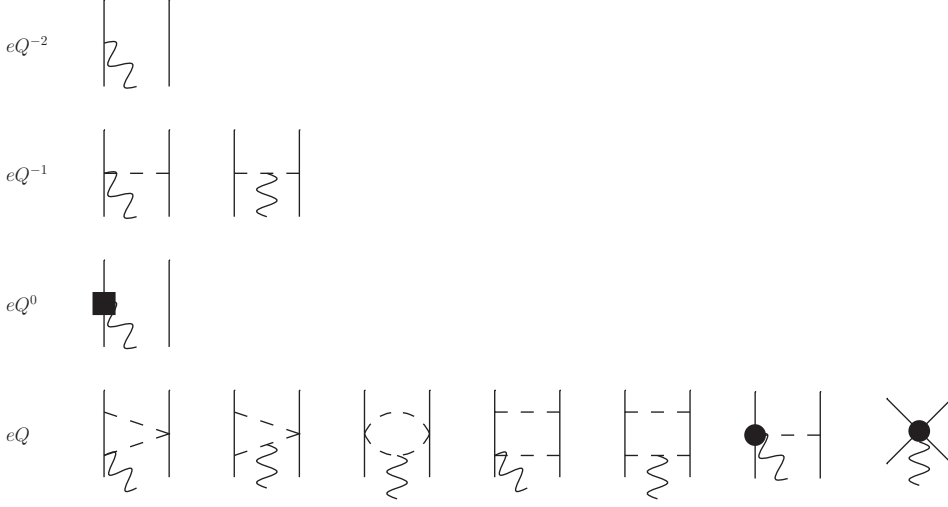


Figure 1: Diagrams illustrating one- and two-body current operators entering at LO (eQ^{-2}), NLO (eQ^{-1}), N2LO (eQ^0), N3LO (eQ^1). The square represents the relativistic correction to the LO one-body operator, whereas the solid circle is associated with a $\gamma\pi N$ current coupling of order eQ^2 . Nucleons, pions, and photons are denoted by the solid, dashed, and wavy lines, respectively.

and

$$\rho^{(-3)} = e e_{N,1}(q^2) \delta(\mathbf{p}'_2 - \mathbf{p}_2) + 1 \Leftrightarrow 2, \quad (2.5)$$

where m_N is the nucleon mass, $\mathbf{q} = \mathbf{k}_i$ with $i = 1$ or 2 (the δ -functions enforcing overall momentum conservation $\mathbf{q} = \mathbf{k}_1$ have been dropped for simplicity here and in the following),

$$\begin{aligned} e_{N,i}(q^2) &= \frac{G_E^S(q^2) + G_E^V(q^2) \tau_{i,z}}{2}, \\ \mu_{N,i}(q^2) &= \frac{G_M^S(q^2) + G_M^V(q^2) \tau_{i,z}}{2}, \end{aligned} \quad (2.6)$$

and $G_E^{S/V}$ and $G_M^{S/V}$ denote the isoscalar/isovector combinations of the proton and neutron electric (E) and magnetic (M) form factors, normalized as $G_E^S(0) = G_E^V(0) = 1$, $G_M^S(0) = 0.880 \mu_N$, and $G_M^V(0) = 4.706 \mu_N$ in units of the nuclear magneton μ_N . The counting eQ^{-2} (eQ^{-3}) of the leading-order current (charge) operator results from the product of a factor eQ (eQ^0) due to the coupling of the external electromagnetic field to the individual nucleons, and the factor Q^{-3} from the momentum δ -function entering this type of disconnected contributions. Of course, this counting ignores the fact that the nucleon form factors themselves also have a power series expansion in Q . Here, they are taken from fits to elastic electron scattering data off the proton and deuteron [12]—specifically, the Höhler parametrization [13]—rather than derived consistently in chiral perturbation theory (χ PT) [14].

We refer to Refs. [8, 9, 15] for the explicit expressions of the current and charge operators up to eQ . In particular, the current operators depend on the known parameters g_A and F_π at next-to-leading order (NLO) and next-to-next-to-next-to-leading order (N3LO), the nucleon's magnetic moments at LO and next-to-next-to-leading order (N2LO). Unknown LEC's enter the isovector (IV) and isoscalar (IS) one-pion-exchange OPE current at N3LO. The IV piece of the OPE current at N3LO

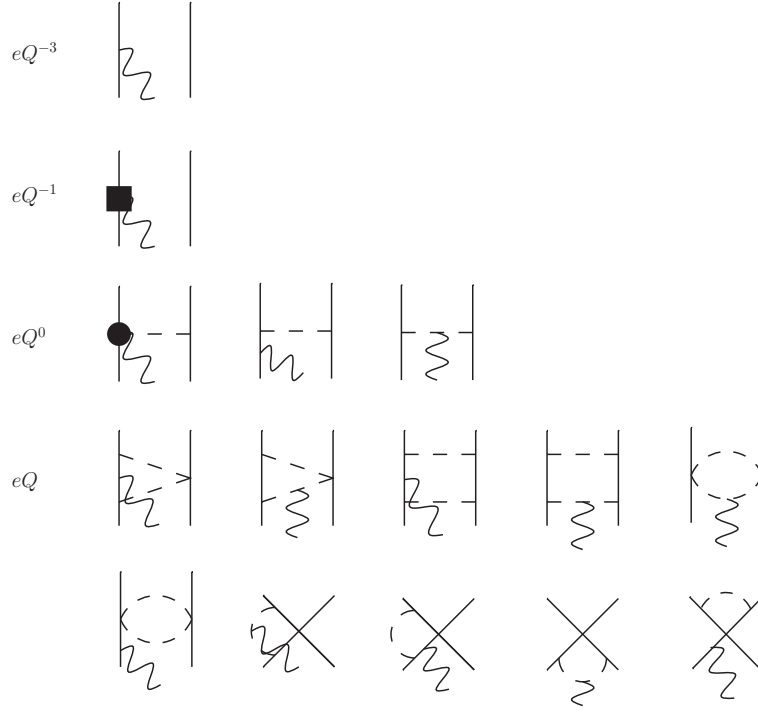


Figure 2: Diagrams illustrating one- and two-body charge operators entering at LO (eQ^{-3}), N2LO (eQ^{-1}), N3LO (eQ^0), N4LO (eQ^1). The square represents the relativistic correction to the LO one-body operator, whereas the solid circle is associated with a $\gamma\pi N$ charge coupling of order eQ . Nucleons, pions, and photons are denoted by the solid, dashed, and wavy lines, respectively.

is given by

$$\mathbf{j}_{\text{b,IV}}^{(1)} = ie \frac{g_A}{F_\pi^2} \frac{G_{\gamma N\Delta}(q^2)}{\mu_{\gamma N\Delta}} \frac{\boldsymbol{\sigma}_2 \cdot \mathbf{k}_2}{\omega_{k_2}^2} \left[d'_8 \boldsymbol{\tau}_{2,z} \mathbf{k}_2 - d'_{21} (\boldsymbol{\tau}_1 \times \boldsymbol{\tau}_2)_z \boldsymbol{\sigma}_1 \times \mathbf{k}_2 \right] \times \mathbf{q} + 1 \Leftrightarrow 2, \quad (2.7)$$

and depends on the LEC's d'_8 and d'_{21} . These LEC's can be related [8] to the N - Δ transition axial coupling constant and magnetic moment (denoted as $\mu_{\gamma N\Delta}$) in a resonance saturation picture, which justifies the use of the $\gamma N\Delta$ electromagnetic form factor for this term. It is parametrized as

$$G_{\gamma N\Delta}(q^2) = \frac{\mu_{\gamma N\Delta}}{(1 + q^2/\Lambda_{\Delta,1}^2)^2 \sqrt{1 + q^2/\Lambda_{\Delta,2}^2}}, \quad (2.8)$$

where $\mu_{\gamma N\Delta}$ is taken as $3 \mu_N$ from an analysis of γN data in the Δ -resonance region [16]. This analysis also gives $\Lambda_{\Delta,1}=0.84$ GeV and $\Lambda_{\Delta,2}=1.2$ GeV. The IS piece of the OPE current at N3LO depends on the LEC d'_9 ,

$$\mathbf{j}_{\text{b,IS}}^{(1)} = ie \frac{g_A}{F_\pi^2} d'_9 G_{\gamma\pi\rho}(q^2) \boldsymbol{\tau}_1 \cdot \boldsymbol{\tau}_2 \frac{\boldsymbol{\sigma}_2 \cdot \mathbf{k}_2}{\omega_{k_2}^2} \mathbf{k}_2 \times \mathbf{q} + 1 \Leftrightarrow 2, \quad (2.9)$$

and, again in a resonance saturation picture, reduces to the well known $\gamma\pi\rho$ current [8]. Accordingly, we have accounted for the q^2 fall-off of the electromagnetic vertex by including a $\gamma\pi\rho$ form

factor, which in vector-meson dominance is parametrized as

$$G_{\gamma\pi\rho}(q^2) = \frac{1}{1 + q^2/m_\omega^2}, \quad (2.10)$$

m_ω being the ω -meson mass. Further LEC's enter the contact minimal and non minimal currents, denoted by the subscripts "min" and "nm" respectively. They are written as

$$\begin{aligned} \mathbf{j}_{a,\text{min}}^{(1)} = & \frac{ie}{16} G_E^V(q^2) (\boldsymbol{\tau}_1 \times \boldsymbol{\tau}_2)_z \left[(C_2 + 3C_4 + C_7) \mathbf{k}_1 + (C_2 - C_4 - C_7) \mathbf{k}_1 \boldsymbol{\sigma}_1 \cdot \boldsymbol{\sigma}_2 \right. \\ & \left. + C_7 \boldsymbol{\sigma}_1 \cdot (\mathbf{k}_1 - \mathbf{k}_2) \boldsymbol{\sigma}_2 \right] - \frac{ie}{4} e_{N,1}(q^2) C_5 \times (\boldsymbol{\sigma}_1 + \boldsymbol{\sigma}_2) \times \mathbf{k}_1 + 1 \Rightarrow 2, \end{aligned} \quad (2.11)$$

$$\mathbf{j}_{a,\text{nm}}^{(1)} = -ie \left[G_E^S(q^2) C'_{15} \boldsymbol{\sigma}_1 + G_E^V(q^2) C'_{16} (\boldsymbol{\tau}_{1,z} - \boldsymbol{\tau}_{2,z}) \boldsymbol{\sigma}_1 \right] \times \mathbf{q} + 1 \Rightarrow 2, \quad (2.12)$$

where the LEC's C_1, \dots, C_7 , which also enter the two-nucleon contact potential, have been constrained by fitting np elastic scattering data and the deuteron binding energy. We take their values from the Machleidt and Entem 2011 review paper [17]. The LEC's C'_{15} and C'_{16} (and d'_8, d'_9 , and d'_{21} discussed above) are determined by fitting measured photo-nuclear observables of the $A = 2$ and 3 systems.

Regarding the charge operators, we want to point out that the specific form of the N3LO charge operator depends on the non-unique off-the-energy shell prescription adopted for the non-static piece in OPE potential [9]. The same applies to part of next-to-next-to-next-to-next-to-leading order (N4LO) contributions. However, different forms of these operators due to different off-the-energy shell prescriptions in the non-static OPE and two-pion-exchange (TPE) potentials are related to each other by unitary transformation [9, 15]. This implies that predictions for physical observables, such as the few-nucleon charge form factors, will remain unaffected by the non-uniqueness associated with the off-the-energy shell effects. We also emphasize that, up to N4LO, charge operators do not have any unknown LEC's. This is in line with the fact that the loop integrals entering the non-vanishing charge diagrams at N4LO are individually ultra-violet divergent, but their sum is finite, i.e. the divergencies cancel out.

3. Electromagnetic form factors of the deuteron and the trinucleons

The deuteron charge (G_C), magnetic (G_M), and quadrupole (G_Q) form factors are obtained from [18]

$$G_C(q) = \frac{1}{3} \sum_{M=\pm 1,0} \langle d; M | \rho(q\hat{\mathbf{z}}) | d; M \rangle, \quad (3.1)$$

$$G_M(q) = \frac{1}{\sqrt{2}\eta} \text{Im}[\langle d; 1 | j_y(q\hat{\mathbf{z}}) | d; 0 \rangle], \quad (3.2)$$

$$\begin{aligned} G_Q(q) = & \frac{1}{2\eta} [\langle d; 0 | \rho(q\hat{\mathbf{z}}) | d; 0 \rangle \\ & - \langle d; 1 | \rho(q\hat{\mathbf{z}}) | d; 1 \rangle], \end{aligned} \quad (3.3)$$

where $|d; M\rangle$ is the deuteron state with spin projection $J_z = M$, ρ and j_y denote, respectively, the charge operator and y component of the current operator, the momentum transfer \mathbf{q} is taken along

the z -axis (the spin quantization axis), and $\eta = (q/2m_d)^2$ (m_d is the deuteron mass). They are normalized as

$$G_C(0) = 1, G_M(0) = (m_d/m_N)\mu_d, G_Q(0) = m_d^2 Q_d, \quad (3.4)$$

where μ_d and Q_d are the deuteron magnetic moment (in units of μ_N) and quadrupole moment, respectively. Expressions relating the form factors to the measured structure functions A and B , and tensor polarization T_{20} are given in Ref. [18]. The charge and magnetic form factors of the trinucleons are derived from

$$F_C(q) = \frac{1}{Z} \langle + | \rho(q\hat{\mathbf{z}}) | + \rangle, \quad (3.5)$$

$$F_M(q) = -\frac{2m_N}{q} \text{Im}[\langle - | j_y(q\hat{\mathbf{z}}) | + \rangle], \quad (3.6)$$

with the normalizations

$$F_C(0) = 1, \quad F_M(0) = \mu, \quad (3.7)$$

where μ is the magnetic moment (in units of μ_N). Here $|\pm\rangle$ represent either the ${}^3\text{He}$ state or ${}^3\text{H}$ state in spin projections $J_z = \pm 1/2$. The calculations are carried out in momentum space [18] and use wave functions derived from either chiral or conventional two- and three-nucleon potentials obtained with the hyperspherical harmonics (HH) technique [19]. The relevant matrix elements are evaluated with Monte Carlo methods.

4. Results

The deuteron $A(q)$ structure function and tensor polarization $T_{20}(q)$, obtained with the chiral and AV18 potentials and cutoff parameters $\Lambda = 500$ MeV and 600 MeV, are compared to data in Fig. 3, top panels. The calculations are performed at LO and with inclusion of charge operators up to N3LO (TOT). The remaining charge operators at N4LO, being isovector, do not contribute to these observables. Predictions corresponding to cutoffs Λ in the range 500–600 MeV are displayed by the bands. The structure function $B(q)$ and magnetic form factor $G_M(q)$, obtained with the AV18 and chiral potentials, and currents at LO and by including corrections up to N3LO, are compared to data in Fig. 4. There is generally good agreement between theory and experiment for q values up to $\simeq 2 \text{ fm}^{-1}$.

The calculated charge form factors of ${}^3\text{He}$ and ${}^3\text{H}$, and their isoscalar and isovector combinations $F_C^S(q)$ and $F_C^V(q)$, normalized, respectively, to 3/2 and 1/2 at $q = 0$, are compared to data in Fig. 5. The agreement between theory and experiment is excellent for $q \lesssim 2.5 \text{ fm}^{-1}$. At larger values of the momentum transfer, there is a significant sensitivity to cutoff variations in the results obtained with the chiral potentials. This cutoff dependence is large at LO and is reduced, at least in ${}^3\text{He}$, when corrections up to N4LO are included. These corrections have opposite sign than the LO, and tend to shift the zeros in the form factors to lower momentum transfers, bringing theory closer to experiment in the diffraction region. Finally, the magnetic form factors of ${}^3\text{He}$ and ${}^3\text{H}$ and their isoscalar and isovector combinations $F_M^S(q)$ and $F_M^V(q)$, normalized respectively as μ_S and μ_V at $q = 0$, at LO and with inclusion of corrections up to N3LO in the current, are displayed in Fig. 6. For $q \lesssim 2 \text{ fm}^{-1}$ there is excellent agreement between the present χEFT predictions and experiment. However, as the momentum transfer increases, even after making allowance for the

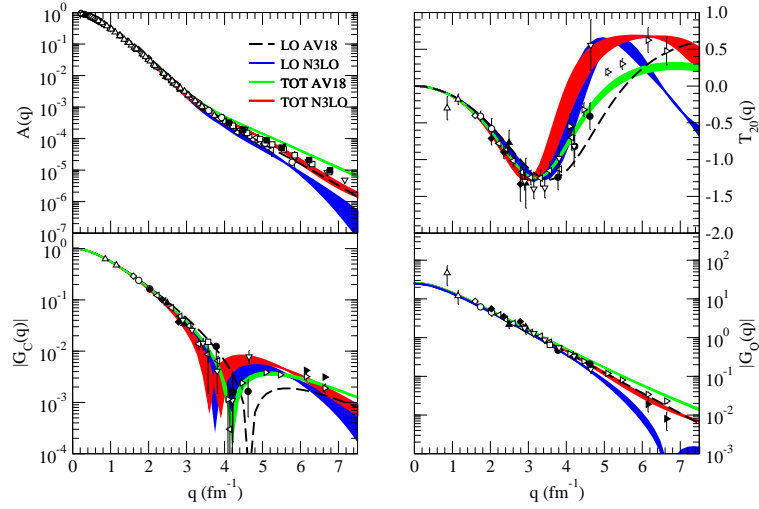


Figure 3: The deuteron $A(q)$ structure function and tensor polarization $T_{20}(q)$ (top panels), and charge and quadrupole form factors $G_C(q)$ and $G_Q(q)$ (bottom panels), obtained at LO and with inclusion of charge operators up to N3LO (TOT), is compared with experimental data from Refs. [20-41]. Predictions corresponding to cutoffs Λ in the range 500–600 MeV are displayed by the bands.

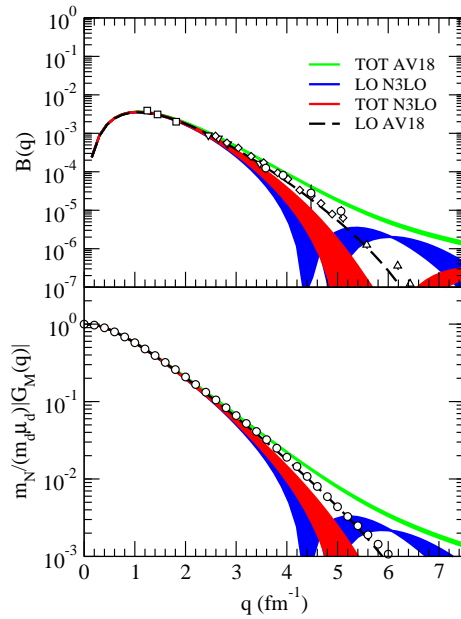


Figure 4: The deuteron $B(q)$ structure function (top panel) and magnetic form factor $G_M(q)$ (bottom panel), obtained at LO and with inclusion of current operators up to N3LO (TOT), is compared with the experimental data from Refs. [20, 26, 42, 27, 43, 44]. Predictions corresponding to cutoffs Λ in the range 500–600 MeV are displayed by the bands.

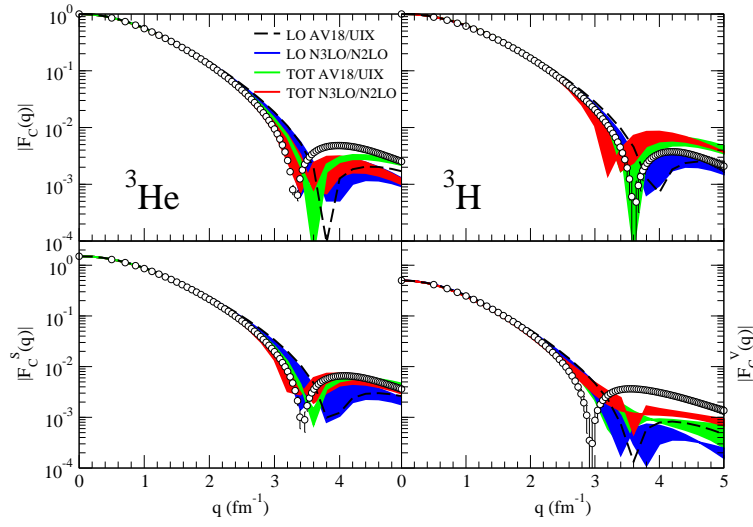


Figure 5: ^3He and ^3H charge form factors (top panels), and their isoscalar and isovector combinations (bottom panels), obtained at LO and with inclusion of charge operators up to N4LO (TOT), is compared with experimental data [45]. Predictions corresponding to cutoffs Λ in the range (500–600) MeV are displayed by the bands.

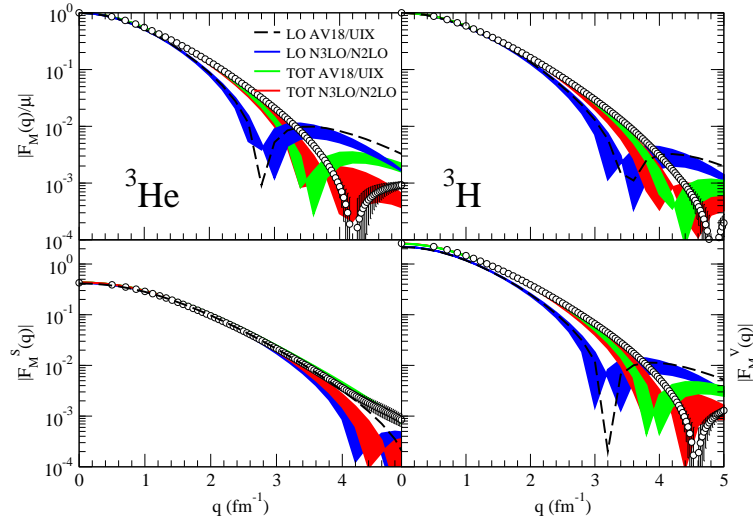


Figure 6: The ^3He and ^3H magnetic form factors (top panels), and their isoscalar and isovector combinations (bottom panels), obtained at LO are compared with experimental data [45]. Predictions relative to cutoffs Λ in the range (500–600) MeV are displayed by the bands.

significant cutoff dependence, theory tends to underestimate the data, in particular it predicts the zeros in both form factors occurring at significantly lower values of q than observed. Thus, the first diffraction region remains problematic for the present theory, confirming earlier conclusions derived from studies in the conventional framework [46, 47].

5. Conclusions

We have provided predictions for the elastic form factors of the deuteron and trinucleons. The wave functions describing these nuclei were derived from either χ EFT or conventional two- and three-nucleon potentials using the HH technique. The matrix elements of the χ EFT charge and current operators were evaluated in momentum-space with Monte Carlo methods.

The χ EFT calculations (based on the N3LO potential) and the hybrid ones (based on the AV18) reproduce very well the observed electromagnetic structure of the deuteron for momentum transfers q up to $2\text{--}3\text{ fm}^{-1}$. Static properties, including charge and magnetic radii, have been also investigated in Ref. [15].

Acknowledgments

The work of R.S. is supported by the U.S. Department of Energy, Office of Nuclear Physics, under contract DE-AC05-06OR23177.

References

- [1] S. Weinberg, Phys. Lett. B **251**, 288 (1990); Nucl. Phys. B **363**, 3 (1991); Phys. Lett. B **295**, 114 (1992).
- [2] P.F. Bedaque and U. van Kolck, Ann. Rev. Nucl. Part. Sci. **52**, 339 (2002).
- [3] E. Epelbaum, H.W. Hammer, and U.-G. Meissner, Rev. Mod. Phys. **81**, 1773 (2009).
- [4] R. Machleidt and D. R. Entem, Phys. Rept. **503**, 1 (2011).
- [5] T.-S. Park, D.-P. Min, and M. Rho, Nucl. Phys. A **596**, 515 (1996).
- [6] T.-S. Park, L. E. Marcucci, R. Schiavilla, M. Viviani, A. Kievsky, S. Rosati, K. Kubodera, D.-P. Min, and M. Rho, Phys. Rev. C **67**, 055206 (2003).
- [7] S. Pastore, R. Schiavilla, and J.L. Goity, Phys. Rev. C **78**, 064002 (2008).
- [8] S. Pastore, L. Girlanda, R. Schiavilla, M. Viviani, and R.B. Wiringa, Phys. Rev. C **80**, 034004 (2009).
- [9] S. Pastore, L. Girlanda, R. Schiavilla, and M. Viviani, Phys. Rev. C **84**, 024001 (2011).
- [10] S. Kölling, E. Epelbaum, H. Krebs, and U.-G. Meissner, Phys. Rev. C **80**, 045502 (2009).
- [11] S. Kölling, E. Epelbaum, H. Krebs, and U.-G. Meissner, Phys. Rev. C **84**, 054008 (2011).
- [12] C.E. Hyde-Wright and K. de Jager, Ann. Rev. Nucl. Part. Sci. **54**, 217 (2004).
- [13] G. Höhler *et al.*, Nucl. Phys. B **114**, 505 (1976).
- [14] B. Kubis and U.-G. Meissner, Nucl. Phys. A **679**, 698 (2001).

- [15] M. Piarulli, L. Girlanda, L. E. Marcucci, S. Pastore, R. Schiavilla, and M. Viviani, *Phys. Rev. C* **87**, 014006 (2013).
- [16] C.E. Carlson, *Phys. Rev. D* **34**, 2704 (1986).
- [17] D. R. Entem and R. Machleidt, *Phys. Rev. C* **68**, 041001(R) (2003).
- [18] R. Schiavilla and V.R. Pandharipande, *Phys. Rev. C* **65**, 064009 (2002).
- [19] A. Kievsky *et al.*, *J. Phys. G: Nucl. Part. Phys.* **35**, 063101 (2008).
- [20] C.D. Buchanan and M.R. Yearian, *Phys. Rev. Lett.* **15**, 303 (1965).
- [21] D. Benaksas, D. Drickey, and D. Frèrejacque, *Phys. Rev.* **148**, 1327 (1966).
- [22] J.E. Elias *et al.*, *Phys. Rev.* **177**, 2075 (1969).
- [23] S. Galster *et al.*, *Nucl. Phys. B* **32**, 221 (1971).
- [24] R.W. Berard *et al.*, *Phys. Lett. B* **47**, 355 (1973).
- [25] R.G. Arnold *et al.*, *Phys. Rev. Lett.* **35**, 776 (1975).
- [26] G.G. Simon, C. Schmitt, and V.H. Walther, *Nucl. Phys. A* **364**, 285 (1981).
- [27] R. Cramer *et al.*, *Z. Phys. C* **29**, 513 (1985).
- [28] S. Platchkov *et al.*, *Nucl. Phys. A* **510**, 740 (1990).
- [29] D. Abbott *et al.*, *Phys. Rev. Lett.* **82**, 1379 (1999).
- [30] L.C. Alexa *et al.*, *Phys. Rev. Lett.* **82**, 1374 (1999).
- [31] M. E. Schulze *et al.*, *Phys. Rev. Lett.* **52**, 597 (1984).
- [32] I. The *et al.*, *Phys. Rev. Lett.* **67**, 173 (1991).
- [33] C. Zhang *et al.*, *Phys. Rev. Lett.* **107**, 252501 (2011).
- [34] V.F. Dmitriev *et al.*, *Phys. Lett. B* **157**, 143 (1985).
- [35] B.B. Wojtsekhowski *et al.*, *Pis'ma Zh. Eksp. Teor. Fiz.* **43**, 567 (1986).
- [36] R. Gilman *et al.*, *Phys. Rev. Lett.* **65**, 1733 (1990).
- [37] D.M. Nikolenko *et al.*, *Phys. Rev. Lett.* **90**, 072501 (2003).
- [38] B. Boden *et al.*, *Z. Phys. C* **49**, 175 (1991).
- [39] M. Ferro-Luzzi *et al.*, *Phys. Rev. Lett.* **77**, 2630 (1996).
- [40] M. Bouwhuis *et al.*, *Phys. Rev. Lett.* **82**, 3755 (1999).
- [41] D. Abbott *et al.*, *Phys. Rev. Lett.* **84**, 5053 (2000).
- [42] S. Auffret *et al.*, *Phys. Rev. Lett.* **54**, 649 (1985).
- [43] P. E. Bosted *et al.*, *Phys. Rev. C* **42**, 38 (1990).
- [44] I. Sick, *Prog. Part. Nucl. Phys.* **47**, 245 (2001).
- [45] A. Amroun *et al.*, *Nucl. Phys. A* **579**, 596 (1994).
- [46] L.E. Marcucci, D.O. Riska, and R. Schiavilla, *Phys. Rev. C* **58**, 3069 (1998).
- [47] L.E. Marcucci, M. Viviani, R. Schiavilla, A. Kievsky, and S. Rosati, *Phys. Rev.* **72**, 014001 (2005).